CHAPTER 3

A SYSTEMATIC APPROACH TO FIND SUITABLE BASIS SETS AND FUNCTIONALS FOR BETTER PREDICTION OF MAGNETIC PARAMETERS USING Cu(II) COMPLEXES

INTRODUCTION

In theoretical calculations it is the most necessary measure to find the most suitable basis set and functional for prediction of results as close as experimentally achieved results. For further calculations of magnetic properties in transition metal complexes and clusters, we have focussed our study on finding suitable basis set and functional for the prediction of magnetic properties. We have studied some Cu(II) complexes which are structurally variable. These complexes have been widely used as precursors for the synthesis of multimetallic complexes [1,2] or single-molecule magnets (SMMs) [3,4]. In some instances the Cu(II) *bis*(oxamato) complexes which we have taken are used in the area of magnetic superexchange phenomena [5].

In the work presented in Section 3A we have taken mono and bidentate ligands bound Cu(II) complexes viz. $[Cu(acac)_2]$ (**1**), $[Cu(NH3)_4^{+2}]$ (**2**), $[Cu(dtc)_2]$ (**3**), $[Cu(en)_2^{+2}]$ (**4**), $[Cu(gly)_2]$ (**5**), $[Cu(NO_3)_2]$ (**6**) and $[Cu(ox)_2]$ (**7**) where the abbreviations stand for: acac= acetylacetone, dtc= dithiocarbamate, en= ethylenediamine, gly= glycine, ox= oxalate. The experimental g-tensor values of the Cu(II) complexes taken are already established in literature and we have tried to compare our calculated values with the experimental results.

In Section 3B we have studied the Cu(II) *bis*(oxamato) complexes viz., $[Cu(opba)]^{2-}$ (**8**), $[Cu(nabo)]^{2-}$ (**9**), $[Cu(acbo)]^{2-}$ (**10**), $[Cu(npbo)]^{2-}$ (**13**) which are polycyclic benzene rings; then we have taken, $[Cu(pba)]^{2-}$ (**11**) and $[Cu(obbo)]^{2-}$ (**12**). The abbreviations used are: opba=*o*-phenylene-*bis*(oxamato), nabo=2,3-naphthalene-*bis*(oxamato), acbo=2,3-anthrachinone-*bis*(oxamato), npbo=1,8-naphthalene-*bis*(oxamato), pba=propylene-*bis*(oxamato) and obbo=o-benzyl-*bis*(oxamato). These Cu(II) complexes were presented in the work of Björn Bräuer *et al.* [6] employing quantum chemical calculations in TURBOMOLE [7,8] and tried to compare the results using ORCA program package employing the IORA method.

Section 3A   Study of mono and bidentate ligands bound Cu(II) complexes

3A.1   Theory

Divalent copper has d^9 electronic configuration with one unpaired electron and a nuclear spin of 1/2. The g-tensor usually requires an adequate treatment of electron correlation. It is calculated as correction, **Δg**, to the free electron value,

$$g = g_e 1 + \Delta g$$

with **g_e**= 2.002319. Up to the level of second-order perturbation theory, the g-shift **Δg** consists of the relevant Breit–Pauli terms,

$$\Delta g = \Delta g_{SO/OZ} + \Delta g_{RMC} + \Delta g_{GC}$$

of which the "paramagnetic" second-order spin-orbit/orbital Zeeman cross term, **$\Delta g_{SO/OZ}$**, dominates (except for extremely small **Δg** -values). The theory of g-tensor was briefly described in Chapter 1.

Besides, finding suitable basis set for computation of g-tensors we have also studied their hyperfine coupling interaction in the given ligand field environment. Fermi contact (A_{iso}) and spin dipolar hyperfine interaction (A_{dip}) contributes towards the total hyperfine coupling tensor (A_{Tot}). In order to estimate these two parameters in the results *aiso* and *adip* terms are put in the input. The isotropic term (A_{iso}) is actually the combination of the Fermi contact term (A_{FC}) and the pseudo-contact term (A_{PC}) which is actually the spin-orbit correction term. More brief explanation of the hyperfine coupling is already discussed in Chapter 1.

$$A_{iso} = A_{FC} + A_{PC}$$

Mathematically the following equation describes the contribution of A_{iso} and A_D towards the total hyperfine coupling constant:

$$A_{iso} = \frac{A_{11} + A_{22} + A_{33}}{3}$$

$$A_{D,x} = A_{11} - A_{iso}$$

$$A_{D,y} = A_{22} - A_{iso}$$

$$A_{D,z} = A_{33} - A_{iso}$$

3A.2   Computational Details

In this work the molecules were optimized using Gaussian 09 program [9] and the g-tensors were calculated using the ORCA program [10]. ORCA is a state-of-the-art electronic structure program package for the computation of EPR parameters, especially g-tensor and D-tensor. Here we have used the IGLO-III basis set specifically designed for the calculation of NMR and EPR properties.We have done the optimization in Gaussian 09 program package at LAN2DZ/B3LYP [11] level of theory and the single point calculation for g-tensor is done in the ORCA program package. For the study of g-tensor single point calculations were performed on the optimized structures employing different functionals: generalized gradient-approximation PW91 functional, hybrid functional B3LYP and B3PW. We have tried to study the changes in the values of g-tensor in accordance with the different types of functionals used. We have taken four conditions for each complexes:

(i)   in first we have used hybrid functional B3LYP and taken auxiliary basis set def2-TZVP as the basis set.

(ii)   In second condition B3LYP along with EPR-III basis set.

(iii)   In the third circumstance we have taken generalized gradient approximation functional PW91 along with def2-TZVP basis set.

(iv)   And lastly we have studied the condition of PW91 and EPR-III as the basis set.

Besides Kutzelniggs basis set for NMR and EPR calculations viz. IGLO-III has been coupled with B3LYP and BP86 functionals as B3LYP-IGLO-III and BP86-IGLO-III (where BP 86 is Becke '88 exchange and Perdew '86 correlation). Also we have employed the ZORA (zero-order relativistic approximation) to take care of the relativistic effect and paired it up with B3LYP and BP 86 functional. The EPR-III basis

set is called the Barone's basis set and it is specifically used for calculation of magnetic parameters.

All the hyperfine calculations are performed at DFT level of theory. For efficient optimization of geometry use of analytic gradient is necessary. In order to avoid the build-up of too much numerical noise, accurate and faster convergence *TightSCF* is included. To describe the core density accurately the integration grid is kept very large. This gives well converged final calculation also in case of optimization. For single point calculation we have implemented DFT-based perturbational method. This can evaluate the correction of spin-orbit interaction towards the hyperfine coupling constant since for heavier elements contribution of the second order contribution of the hyperfine coupling from the spin-orbit coupling (SOC) must also be taken into consideration. For this the keyword *aorb* is included in the input. From this we can get the interpretation of spin polarization effects by including the unrestricted Kohn-Sham treatment as revealed from the work of F. Neese [12].

We have used the generalized gradient approximation BP functional. In this case B3LYP is avoided because it relentlessly overestimates the hyperfine coupling constant [13]. The variationally stable ZORA method (zeroth-order regular approximation) [14] is used for the inclusion of relativistic effect. It is the most expedient and approximate relativistic method. Hence we have done ZORA in density functional framework. By studying the relation between the electronic structure and the hyperfine couplings would help in looking for improved theoretical approaches in this regard.
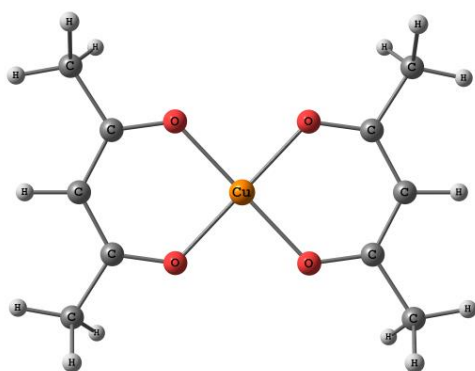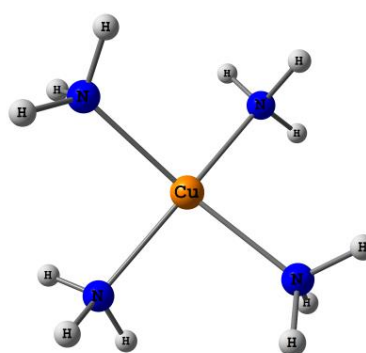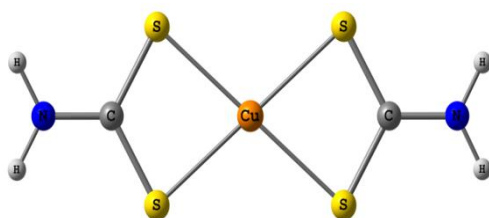
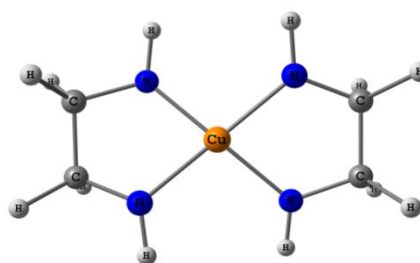## 3A.3   Results and discussion

(1) [Cu(acac)$_2$]   (**2**)   [Cu(NH3)$_4$$^{+2}$]

(**3**)   [Cu(dtc)$_2$]

(**4**)   [Cu(en)$_2$$^{+2}$]
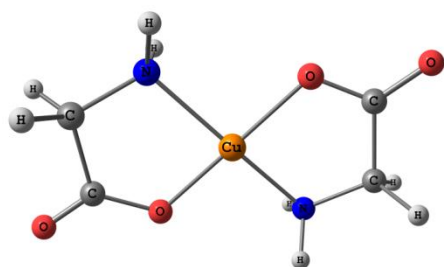
(**5**)   [Cu(gly)$_2$]   (**6**)   [Cu(NO$_3$)$_2$]
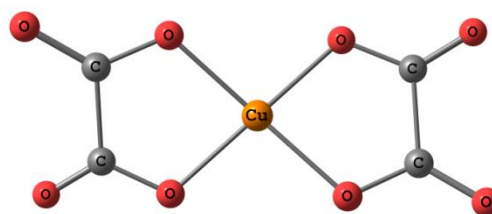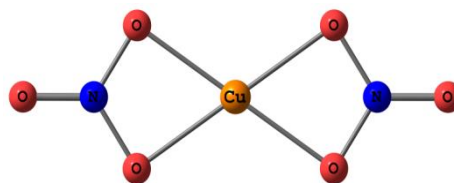
(**7**)   [Cu(ox)$_2$]

Figure 3A.1: Optimized Cu(II) complexes

Table 3A.1: Comparison of experimental and theoretical g-tensors

Sl. No.	Complex	Experimental g-tensor	Calculated g-tensor		Reference
(1)	$[Cu(acac)_2]$	2.166	B3LYP	2.029	15
			EPR-III /B3LYP	2.103	
			PW91	2.027	
			EPR-III /PW91	2.097	
(2)	$[Cu(NH_3)_4]^{+2}$	2.111	B3LYP	2.097	16
			EPR-III /B3LYP	2.116	
			PW91	2.049	
			EPR-III /PW91	2.107	
(3)	$[Cu(dtc)_2]$	2.041	B3LYP	2.030	17,18,19
			EPR-III /B3LYP	2.036	
			PW91	2.029	
			EPR-III /PW91	2.032	
(4)	$[Cu(en)_2]^{+2}$	2.101	B3LYP	2.089	20
			EPR-III /B3LYP	2.095	
			PW91	1.095	
			EPR-III /PW91	2.086	
(5)	$[Cu(gly)_2]$	2.123	B3LYP	2.093	16
			EPR-III /B3LYP	2.114	
			PW91	2.053	
			EPR-III /PW91	2.078	
(6)	$[Cu(ox)_2]$	2.111	B3LYP	2.578	21
			EPR-III /B3LYP	2.612	
			PW91	2.412	
			EPR-III /PW91	2.609	
(7)	$[Cu(NO_3)_2]$	2.632	B3LYP	2.085	22
			EPR-III /B3LYP	2.109	
			PW91	2.086	
			EPR-III /PW91	2.097	

Table 3A.1 reveals compared values of experimental and theoretical g-tensors. As we have earlier mentioned that the optimized geometries are used to calculate the g-tensor values and compare the results obtained using different basis sets and functionals. We have considered all the g-values along the three coordinates. The shifts are different for g_x, g_y and the g_z. Our main focus is to find out which pair of basis set and functional gives the best g-values closer to the experimentally available data.

From the table it is revealed that the basis set EPR-III gives value closer to the experimental results as compared to the def2-TZVP basis set. It is obvious that EPR-III gives better results because it is extensively and exclusively used for calculation of magnetic parameters g-tensor, in our case, besides other parameters like D-tensor, hyperfine coupling constants. When the hybrid functional is compared with the GGA functional of PW91 we obtain that the B3LYP functional gives better results because hybrid functionals give more rational metal-ligand covalencies and better effective energy denominators. Hence it is revealed that the hybrid functionals are better in prediction of g-tensors. Next we have considered the pairing up of both the hybrid and the GGA functionals with the EPR-III basis set. This combination gives values closer to the experimental values. But the best results are obtained from the combination of hybrid functional and the EPR-III basis sets. Therefore, we can say that the EPR-III/B3LYP level gives good results when compared with the experimental values.

Table 3A.2: Contribution of isotropic (A_{iso}) and dipolar (A_{dip})

Sl. No.	Complexes	Isotropic hyperfine coupling contribution, (A_{iso}) (in MHz)	Spin dipolar hyperfine coupling contribution, (A_{dip}) (in MHz)	Total hyperfine coupling constants (A_{Tot}) (in MHz)
(1)	$[Cu(acac)_2]$	-77.343	-154.687	-232.03
(2)	$[Cu(NH3)_4]^{+2}$	186.799	379.599	566.398
(3)	$[Cu(dtc)_2]$	-108.807	-217.615	-326.423
(4)	$[Cu(en)_2]^{+2}$	-68.670	-137.341	-206.011
(5)	$[Cu(gly)_2]$	-232.193	-464.388	-696.581
(6)	$[Cu(NO_3)_2]$	-95.650	-191.3	-286.951
(7)	$[Cu(ox)_2]$	-293.113	-586.227	-879.34

Table 3A.2 shows the contribution of isotropic and dipolar part towards the total hyperfine A_{Tot}. Since the complexes are of 1st row transition elements the spin-orbit part (A_{PC}) do not contribute significantly towards the isotropic hyperfine coupling interaction

A_{iso}. Hence the pseudo-contact (A_{PC}) term is negligible and hence the isotropic hyperfine A_{iso} is equivalent to the Fermi contact term A_{FC}. But in these complexes $A_{PC} \sim 0$. It is also seen in the calculations.

When we used the hybrid functional it was seen that the A_{iso} is overestimated for these complexes. Also the spin polarization is overestimated and this leads to greater A_{FC} which in turn causes increase in A_{iso}. Hence for these Co complexes the hybrid functional seems not much favourable than the GGA functional. In all the cases the spin-orbit correction term A_{PC} has the opposite sign and considerably negligible as compared to the Fermi contact term. However, the hybrid functional shows results where the contribution of the spin-orbit effect is higher and this is erroneous and hence we completely ignore the calculations doing using the hybrid functional B3LYP. While the GGA functional gives result in closer agreement with the experimental values and in accordance with the well-established fact that the contribution of the isotropic part A_{iso} is less than that of the dipolar interaction parameter A_{dip}.

Table 3A.3: Contribution of the pseudo-contact (A_{PC}) term towards the isotropic hyperfine (A_{iso}) parameter

Sl. No.	Complexes	Spin-orbit hyperfine coupling contribution, (A_{PC}) (in MHz)	Fermi-contact hyperfine coupling contribution, (A_{FC}) (in MHz)	Total Isotropic hyperfine coupling constants (A_{iso}) (in MHz)
(1)	[Cu(acac)$_2$]	0	-77.343	-77.343
(2)	[Cu(NH3)$_4$]$^{+2}$	-0.003	186.802	186.799
(3)	[Cu(dtc)$_2$]	0	-108.807	-108.807
(4)	[Cu(en)$_2$]$^{+2}$	-0.002	-68.672	-68.670
(5)	[Cu(gly)$_2$]	-0.001	-232.194	-232.193
(6)	[Cu(NO$_3$)$_2$]	0	-108.807	-108.807
(7)	[Cu(ox)$_2$]	-0.003	-293.116	-293.113

The density functional calculations based on perturbational methods may overestimate or underestimate the isotropic effect depending on the type of functional used. However, it is found that the use of ZORA approximation enhances the simultaneous inclusion of spin polarization and spin-orbit coupling. From table 3A.3 it is seen that the isotropic Fermi Contact hyperfine is dominant. This is a highly singular property that depends on the spin-density of the nucleus of the corresponding metal ion. Therefore, we can conclude from this that a high accuracy wave function is required in the vicinity of the concerned nucleus. Hence a flexible functional is used for this purpose.

Section 3B   Study of basis sets and functionals in Cu(II) *bis*(oxamato) complexes

3B.1   Theory

This set of Cu(II) *bis*(oxamato) complexes and their structurally isomorphic Ni(II) complexes were experimentally synthesized and their magnetic properties like g-tensor, hyperfine coupling constants etc. were reported in literature. Moreover, there are cases where Cu(II)-*bis*(oxamato) complexes are used in the area of magnetic superexchange phenomena [23]. Theoretical methods such as quantum mechanical methods (QM), Hartree-Fock (HF) method, post HF and the density functional method (DFT) allows for economical treatment of the electron correlation and provides a strong comparison for the theoretical and the corresponding experimental values. There are many evidences where the QM methods have been comprehensively used for the assessment of EPR parameters [24−28]. In these Cu(II)-*bis*(oxamato) complexes Cu has d^9 electronic configuration. Divalent Cu possesses one unpaired electron and a spin of 3/2. The divalent copper is paramagnetic in nature and hence EPR is the best method for evaluation of its first coordination shell and the environment. Cu(II) in ligand field environment is split into five 3d degenerate orbitals and this characteristically leads to Cu g-tensor values [29] which are generally anisotropic. This is so because anisotropy is dependent on the orientation of the z-axis of the complex relative to the applied magnetic field. There are many such cases reported which claim to be rigorous and efficient DFT based parameterized approaches for accurate estimation g-tensor and comparing them with the experimentally derived values. Such approaches may vary from two-component spin-restricted formalism [30] to various types of models which rely on second-order perturbation theory in ne-component scheme [31−33]. Since spin-orbit coupling comprises the most dominant feature in determining the g-tensor, therefore the most successful approach is based on an effective one-electron approximation to the spin-orbit coupling operator and this method is extensively used both as semi-empirical and DFT-based methods [34−37].

3B.2   Computational Details

The optimization of the Cu(II) *bis*(oxamato) complexes is done in the ORCA program package [38]. The Cu(II) ions have been optimized at SDD [39,40] basis set and auxiliary basis set for Coulomb fitting def2-TZVP/J and Ahlrich basis set def2-TZVP [41,42] for the remaining atoms for example, C, H, N, O, etc. The functional used was local and gradient corrected BP functional. In the SCF part we have used *TightSCF* which is set as default in ORCA to avoid buildup of too much numerical noise in the gradient. For the spin-orbit coupling contribution we have employed the CP method, i.e. the coupled perturbed approach. The CP method has the advantage over other methods for ZFS like the Pederson-Khanna method and the QRO (quasi-restricted orbitals) approach because the CP method uses revised pre-factors for the spin-flip terms and can solve set of CP equations for the SOC (spin-orbit coupling) perturbation [43].

In this study we have first tried to investigate as to which functional and basis set would be more appropriate for carrying out the further estimation of g-tensors. Hence we have considered the following four schemes: in the first condition:

(i)   we have taken hybrid functional B3LYP and auxiliary basis set def2-TZVP,

(ii)   in the second case we have taken hybrid functional B3LYP paired with EPR-III basis set [44] which has extra flexibility in the core region.

(iii)   In the third circumstance we have taken generalized gradient approximation (GGA) functional PW91 along with def2-TZVP basis set and lastly

(iv)   we have studied the condition of taking PW91 as the functional and the EPR-III as the basis set. EPR-III basis set is the Barone's basis set at triple zeta level. It is exclusively tailored for the calculation of EPR parameters in density functional calculations [45─48].

Here we would carry out a quantitative comparison between the hybrid and the GGA functional in one instance whereas between the conventional and the EPR-III basis set which is tailored specifically for the calculation of EPR parameters.

Single point energy calculation for magnetic parameter g-tensor for each complex is done at SCF level through Coupled-Perturbed SCF equations. The basis set and functional are as mentioned in the four schemes above. The best scheme, i.e. the best

combination of the basis set and the functional is used in further calculation. Thereafter, we have employed a relativistic approximation IORA. Among the several variants of scalar relativistic Hamiltonians to use in all electron calculations IORA [49─51] is one of the most important methods. IORA stands for infinite-order regular approximation. The term IORA was coined by Dyall and van Lenthe [52] in 1999. The spin-free variant of IORA is implemented on ORCA. The quasi-relativistic method which is obtained by using the ZORA ansatz with a fully variational derivation gives the IORA approach. The IORA method gives faster convergence when the IORA energy is subjected to higher-order corrections. This makes the IORA method to be a propitious alternative to traditional approaches within the framework of regular approximations [53]. IORA is a variationally stable method and it can be used as a suitable starting point for the development of second-order regular approximation of NESC (normalized elimination of the small component). Mathematically, the equation for IORA is

$$\hat{H}^{IORA}\Psi^{IORA} = \mathrm{E}^{IORA}\Psi^{IORA}$$

When a new wave function is defined, we have

$$\varphi^{IORA} = \frac{1}{\sqrt{1 + \hat{X}_0^{\dagger}\hat{X}_0}}$$

$$\hat{H}^{IORA}\varphi^{IORA} = \mathrm{E}^{IORA}(1 + \hat{X}_0^{\dagger}\hat{X}_0)\varphi^{IORA}$$

Unlike the IORA method, the ZORA method has the disadvantage that the core levels of heavy elements are not appropriately reproduced. On the other hand, IORA, being of higher order regular approximation appreciably improves the situation by approaching the Dirac eigenvalues much better than the ZORA method. Hence it is seen that the ZORA equation with a modified metric operator yield the IORA form. These types of disadvantages of the ZORA over the IORA method is reflected in the numerical results, which obtained using ZORA method are less agreeable than those obtained using the IORA method. Though IORA has poor gauge invariance, it is corrected by NESC (normalized elimination of small components).
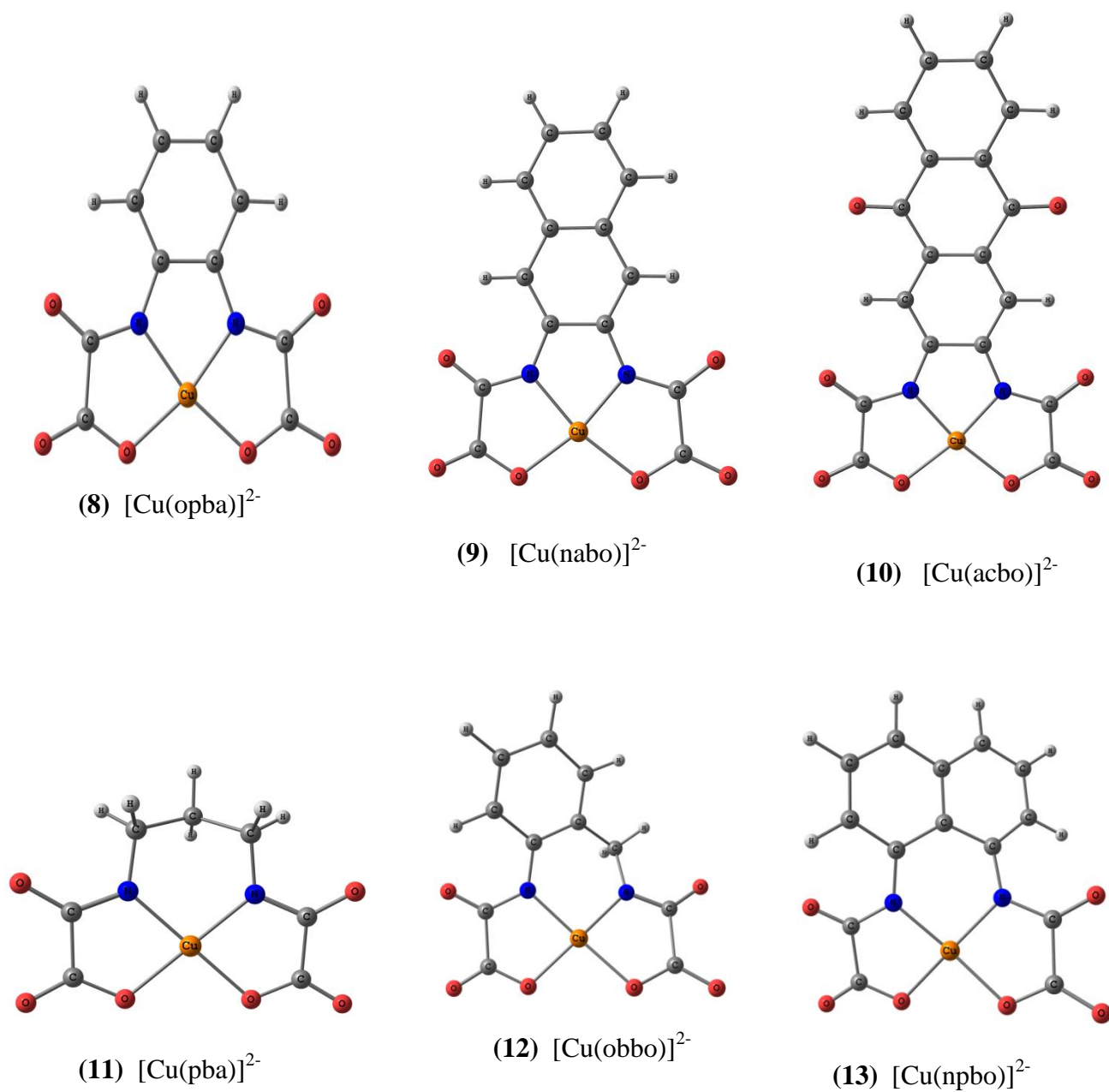
3B.3   Results and discussion

(8) [Cu(opba)]²⁻

(9) [Cu(nabo)]²⁻

(10) [Cu(acbo)]²⁻

(11) [Cu(pba)]²⁻

(12) [Cu(obbo)]²⁻

(13) [Cu(npbo)]²⁻

Figure 3B.1: Optimized structures of Cu(II) *bis*(oxamato) complexes

Table 3B.1: Bond lengths of the Cu(II)-*bis*(oxamato) complexes

Bonds/Complexes	8	9	10	11	12	13
Cu-N1/Å	1.904	1.942	1.939	2.002	1.942	1.955
Cu-N2/Å	1.905	1.942	1.953	1.909	1.941	1.955
Cu-O1/Å	1.959	1.988	1.968	1.966	1.996	2.002
Cu-O2/Å	1.963	1.988	1.966	2.010	1.992	2.001

Table 3B.1 shows the bond lengths between the metal atom Cu and the ligand which is coordinating through two N and two O atoms. The Cu-N bond length is shorter than the Cu-O bond length. However no inference can be drawn from the relation between the metal-ligand bond lengths and the g-tensor values. But it is observed that the complex $[Cu(pba)]^{2-}$ which has highest g-tensor value along with $[Cu(obbo)]^{2-}$, has the longest Cu-N bond length as well as one of the longest Cu-N bond lengths.

The comparison between the hybrid (B3LYP) and the GGA functional (PW91) shows that the hybrid functional B3LYP gives g-tensor values closer than the experimental ones. This can be attributed to the fact that the hybrid functional gives more rational metal-ligand covalencies and better effective energy denominators. Next we have considered the pairing up of both the hybrid and GGA functional along with the EPR-III basis set respectively. The best result is obtained by combination of hybrid B3LYP and the EPR-III basis set. This implies that the basis set exclusively tailored for magnetic parameters have been found satisfactory in case with these Cu(II) complexes.

We have compared our calculated g-tensor values obtained from the IORA (NESC) method with the experimental g-values and the theoretical g-values as reported in the Björn Bräuer *et al.* investigation. Table 3B.2 shows the experimental g-tensor values of the Cu(II) *bis*(oxamato) complexes and Table 3B.3 has the compared values of the calculated g-tensor values from the simple quantum chemical investigation done by the Björn Bräuer group and our evaluation of g-tensors done through the IORA method.

Table 3B.2: Experimental g-Tensor Values

Sl. No.	Complexes	Experimental g-Tensor Values			
		g_x	g_y	g_z	g_{iso}
8	$[Cu(opba)]^{2-}$	2.042	2.042	2.184	2.089
9	$[Cu(nabo)]^{2-}$	2.041	2.041	2.180	2.087
10	$[Cu(acbo)]^{2-}$	2.042	2.042	2.186	2.090
11	$[Cu(pba)]^{2-}$	2.045	2.045	2.185	2.092
12	$[Cu(obbo)]^{2-}$	2.042	2.042	2.193	2.092
13	$[Cu(npbo)]^{2-}$	2.040	2.040	2.185	2.088

We can see that the experimental g-tensors range from 2.087 to 2.092 in case of Cu(II) *bis*(oxamato) complexes. This small range of value can be attributed to the same coordinating sphere (N_2O_2) around the Cu(II) ion. The *bis*(oxamato) ligands in these complexes vary only in their substitutional N atoms.It is evident that the g-tensor value is more for distorted complexes rather than the more symmetric **8, 9,** and **12** numbered complexes. This trend of g-tensor decreasing from distorted symmetry to more symmetric complexes is attributed to the increase in the energy separation of the electronic levels when going from the distorted to symmetrical complexes.

**Table 3B.3:** Comparison of g-tensors of quantum mechanical and IORA method

Sl. No.	Complexes	Calculated g-tensors from the reference				Calculated g-tensors from the IORA method			
		g_x	g_y	g_z	g_{iso}	g_x	g_y	g_z	g_{iso}
8	$[Cu(opba)]^{2-}$	2.033	2.035	2.116	2.061	2.043	2.047	2.136	2.075
9	$[Cu(nabo)]^{2-}$	2.034	2.037	2.115	2.062	2.039	2.042	2.123	2.068
10	$[Cu(acbo)]^{2-}$	2.038	2.039	2.131	2.069	2.047	2.046	2.125	2.073
11	$[Cu(pba)]^{2-}$	2.034	2.036	2.119	2.063	2.041	2.042	2.117	2.067

Sl. No.	Complexes	Calculated g-tensors from the reference				Calculated g-tensors from the IORA method			
		g_x	g_y	g_z	g_{iso}	g_x	g_y	g_z	g_{iso}
12	[Cu(obbo)]$^{2-}$	2.038	2.04	2.133	2.070	2.039	2.042	2.136	2.072
13	[Cu(npbo)]$^{2-}$	2.031	2.032	2.105	2.056	2.034	2.037	2.115	2.062

The calculated g-tensor values are much smaller than the experimental values. Another important factor determining the trend of g-tensor in this set of Cu(II) complexes is that the spin population is localized at the Cu(II) ion centre and while the N atoms have higher spin population as compared to the O atom. This fact is attributed to the smaller Cu–N bond lengths and the stronger Cu–N bond. IORA method when paired with the NESC in the modified Dirac equation gives g-tensor values much closer to the experimental g-values. It is also presents values better than the quantum chemical method applied by the Björn Bräuer group using the TURBOMOLE program. However, when only IORA method, not harmonized with the NESC approach give poor g-values. We can say that the NESC method is the projection of the Dirac Hamiltonian onto a set of positive energy (electronic) states, which in turn guarantees its variational stability [54]. The NESC method is formulated in the matrix form and hence, it allows formulation of the regular approximation used, i.e. IORA in this case, within WFT (wave function theory) which is perfectly suited for the use of atomic and molecular calculations in finite basis sets.

(8) [Cu(opba)]$^{2-}$
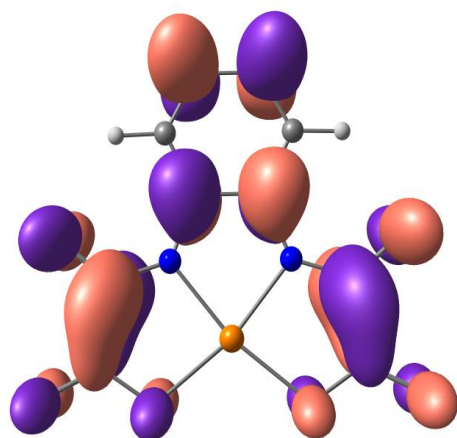
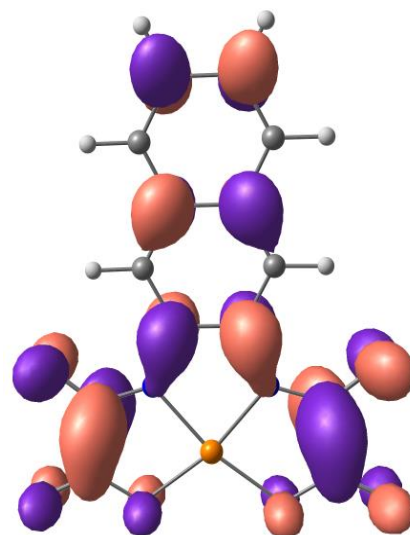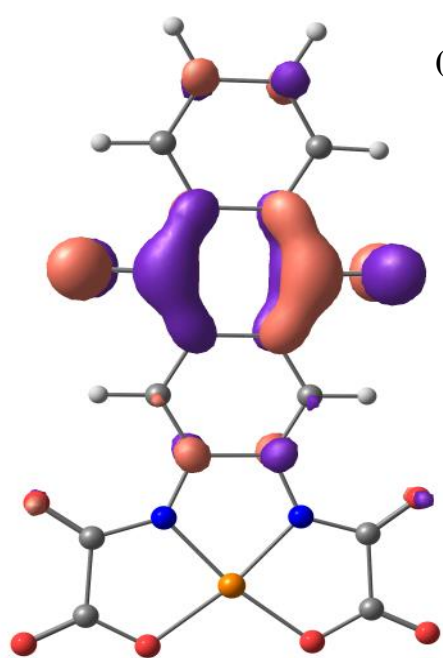**(8)** HOMO
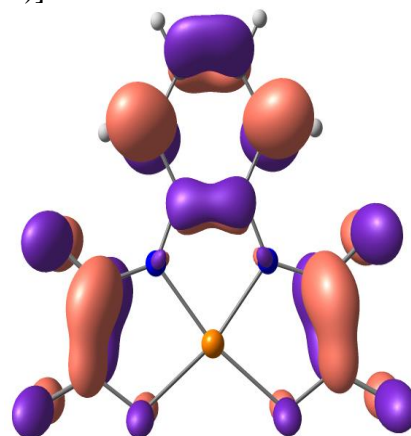
(8) LUMO

(9) [Cu(nabo)]$^{2-}$
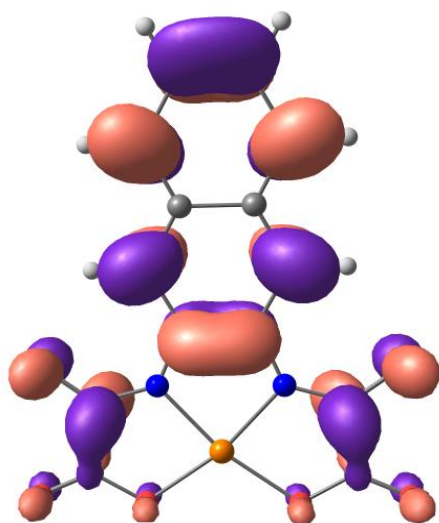
(9) HOMO

(9) LUMO

(10) [Cu(acbo)]$^{2-}$

(10) HOMO
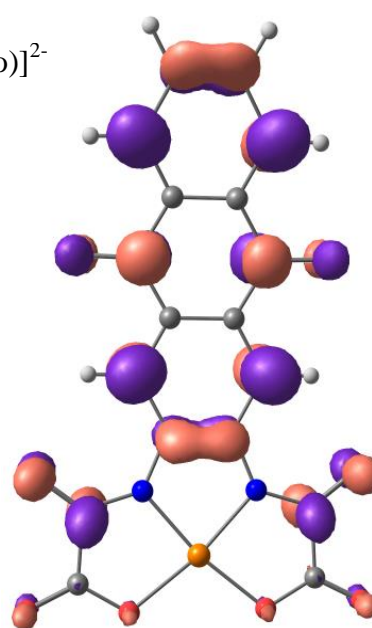
(10) LUMO

(11) [Cu(pba)]$^{2-}$

(11) HOMO

(11) LUMO

(12) [Cu(obbo)]$^{2-}$

(12) HOMO

(12) LUMO

(13) [Cu(npbo)]$^{2-}$
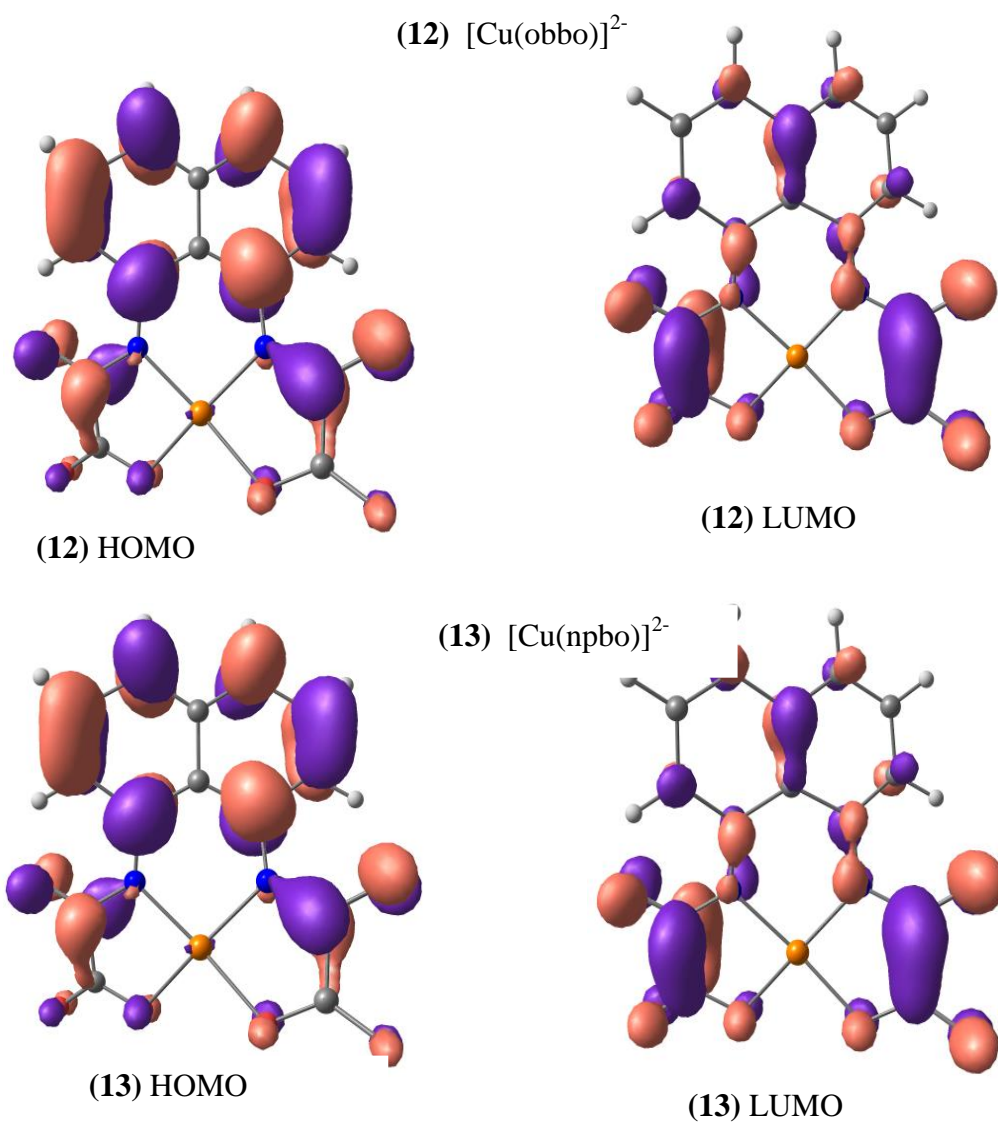

(13) HOMO
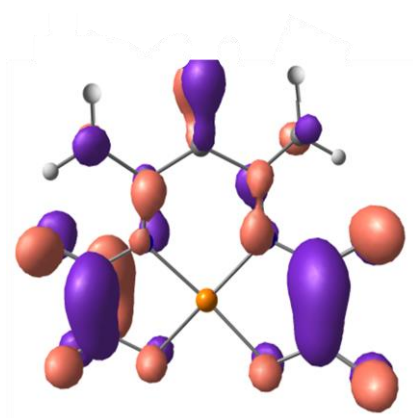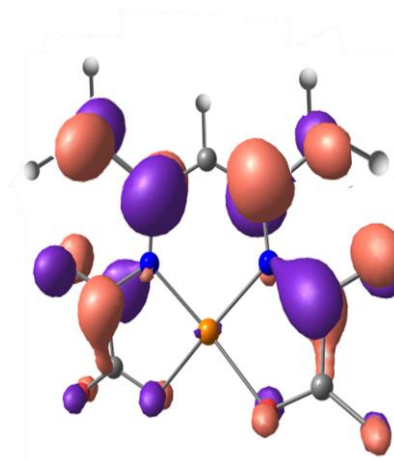
(13) LUMO

Figure 3B.2: FMOs of Cu(II) bis(oxamato) complexes

The study of frontier molecular orbital study of these complexes reveals that the highest HOMO-LUMO gap exists in [Cu(acbo)]$^{2-}$. Here we have employed fixed spin moment, and this establishes a correlation with the frontier orbital study. The total number of electrons is fixed between majority and minority spin channel. The Zeeman term of g-tensor is used to split the chemical potentials into two spin channels. In [Cu(acbo)]$^{2-}$ both the majority and minority spin channels are exposed to a chemical potential difference that generates an effective magnetic field.

REFERENCES

[1]   Frisch, M. J., Trucks, G. W., Schlegel, H. B., Scuseria, G. E., Robb, M. A., Cheeseman, J. R. and Nakatsuji, H. *Gaussian 09, Revision D. 01,* Inc., Wallingford CT, 2013.

[2]   Hay, P. J. and Wadt, W. R. Ab initio effective core potentials for molecular calculations. Potentials for the transition metal atoms Sc to Hg. *The Journal of Chemical Physics,* 82(1):270–283, 1985.

[3]   F. Neese (Max Planck–Institute for Bioinorganic Chemistry), *ORCA, Version 2.9.0*, An ab initio, DFT and semiempirical SCF–MO package –with contributions from U. Becker, D. Bykov, D. Ganyushin, A. Hansen, R. Izsak, D.G. Liakos, C. Kollmar, S. Kossmann, D.A. Pantazis, T. Petrenko, C. Reimann, C. Riplinger, M. Roemelt, B. Sandhöfer, I. Schapiro, K. Sivalingam, F. Wennmohs, B. Wezisla and contributions from collaborators: M. Kállay, S. Grimme, E. Valeev, 2012.

[4]   Rollman,L. D. Ed. *Electron Spin Resonance of Metal Complexes*, page 175. Adam Hilger: London, 1969

[5]   Scholl, H. J. and Hüttermann, J. ESR and ENDOR of copper (II) complexes with nitrogen donors: probing parameters for prosthetic group modeling of superoxide dismutase. *The Journal of Physical Chemistry*, 96(24):9684–9691, 1992.

[6]   Keijzers, C. P., Paulussen, G. F. M. and De Boer, E. ESR Study of copper and silver N, N-dialkyldiselenocarbamates: Part I. Analysis of spectra measured in host lattices with monomeric structures. *Molecular Physics*, 29(4):973-1006, 1975.

[7]   Keijzers, C. P., De Vries, H. J. M. and Van der Avoird, A. Extended Hückel calculation of the electron paramagnetic resonance parameters of copper (II) bis (dithiocarbamate). *Inorganic Chemistry*, 11(6):1338–1343, 1972.

[8]   Geurts, P. J. M., Bouten, P. C. P. and Van der Avoird, A. Hartree-Fock-Slater-LCAO calculations on the Cu (II) bis (dithiocarbamate) complex; Magnetic coupling parameters and optical spectrum. *The Journal of Chemical Physics*, 73(3):1306–1312, 1980.

[9]   Frisch, M. J., Trucks, G. W., Schlegel, H. B., Scuseria, G. E., Robb, M. A., Cheeseman, J. R. and Dapprich, S. *Gaussian 98, Revision A. 9*, Gaussian, Inc. Pittsburgh, 1998.

[10]   Neese, F., Wennmohs, F., Becker, U., Bykov, D., Ganyushin, D., Hansen, A and Pantazis, D. A. *ORCA, Version 3*.0. Institute for physical and theoretical chemistry, Bonn, 2014.

[11]   Hay, P. J. and Wadt, W. R. Ab initio effective core potentials for molecular calculations. Potentials for the transition metal atoms Sc to Hg. *The Journal of Chemical Physics*, 82(1):270–283, 1985.

[12]   Neese, F. Metal and ligand hyperfine couplings in transition metal complexes: The effect of spin-orbit coupling as studied by coupled perturbed Kohn-Sham theory. *The Journal of Chemical Physics*, 118(9):3939–3948, 2003.

[13]   Shiozaki, T. and Yanai, T. Hyperfine coupling constants from internally contracted multireference perturbation theory. *Journal of Chemical Theory and Computation,* 12(9):4347–4351, 2016.

[14]   van Lenthe, E., Van Der Avoird, A. D. and Wormer, P. E. Density functional calculations of molecular hyperfine interactions in the zero order regular approximation for relativistic effects. *The Journal of Chemical Physics*, 108(12):4783–4796, 1998.

[15]   Rollman, L. D., Chan, S. I., InYen, T. F. Ed. *Electron Spin Resonance of Metal Complexes*, page 175. Adam Hilger: London, 1969.

[16]   Scholl, H. J. and Hüttermann, J. ESR and ENDOR of copper (II) complexes with nitrogen donors: Probing parameters for prosthetic group modeling of superoxide dismutase. *The Journal of Physical Chemistry*, 96(24):9684–9691, 1992.

[17]   Keijzers, C. P. and DeBoer, E. ESR of copper and, + dialkyl diselenocarbamates II. Interpretation of spectra measured in host lattices with monomeric structures. *Molecular Physics*, 29:1007, 1975.

[18]   Keijzers, C. P., De Vries, H. J. M. and Van der Avoird, A. Extended Hückel calculation of the electron paramagnetic resonance parameters of copper (II) bis (dithiocarbamate). *Inorganic Chemistry*, 11(6):1338–1343, 1972.

[19]   Geurts, P. J. M., Bouten, P. C. P. and Van der Avoird, A. Hartree-Fock-Slater-LCAO calculations on the Cu (II) bis (dithiocarbamate) complex; Magnetic coupling parameters and optical spectrum. *The Journal of Chemical Physics*, 73(3):1306–1312, 1980.

[20]   Ehsan, M. Q., Ohba, Y., Yamauchi, S. and Iwaizumi, M. EPR and ENDOR study of trigonal bipyramidal copper complexes with a nitrogen donor tripodal ligand. *Bulletin of the Chemical Society of Japan*, 69(8):2201–2209, 1996.

[21]   Yordanov, N. D., Stankova, M. and Shopov, D. EPR study of bis (8-quinolinethiolato) copper (II) and bis (8-quinolinolato) copper (II) complexes. *Chemical Physics Letters*, 39(1):174–176, 1976.

[22]   Ehsan, M. Q., Ohba, Y., Yamauchi, S. and Iwaizumi, M. EPR and ENDOR study of trigonal bipyramidal copper complexes with a nitrogen donor tripodal ligand. *Bulletin of the Chemical Society of Japan*, 69(8):2201–2209, 1996.

[23]   Costa, R., Garcia, A., Sanchez, R., Ribas, J., Solans, X. and Rodriguez, V. Synthesis, structure and magnetic properties of trinuclear complexes of copper (II) with different amines as terminal ligands. *Polyhedron*, 12(22):2697–2704, 1993.

[24]   Peisach, J. and Blumberg, W. E. Structural implications derived from the analysis of electron paramagnetic resonance spectra of natural and artificial copper proteins. *Archives of Biochemistry and Biophysics*, 165(2):691–708, 1974.

[25]   Bruschi, M., De Gioia, L., Mitrić, R., Bonačić–Koutecký, V. and Fantucci, P. A DFT study of EPR parameters in Cu (II) complexes of the octarepeat region of the prion protein. *Physical Chemistry Chemical Physics*, 10(31):4573–4583, 2008.

[26]   Pierloot, K., Delabie, A., Groothaert, M. H. and Schoonheydt, R. A. A reinterpretation of the EPR spectra of Cu (II) in zeolites A, Y and ZK4, based on ab initio cluster model calculations. *Physical Chemistry Chemical Physics*, 3(11):2174–2183, 2001.

[27]   Groothaert, M. H., Pierloot, K., Delabie, A. and Schoonheydt, R. A. Identification of Cu (II) coordination structures in Cu–ZSM–5, based on a

DFT/ab initio assignment of the EPR spectra. *Physical Chemistry Chemical Physics*, 5(10):2135–2144, 2003.

[28] Delabie, A., Pierloot, K., Groothaert, M. H., Weckhuysen, B. M. and Schoonheydt, R. A. The siting of Cu (II) in mordenite: a theoretical spectroscopic study. *Physical Chemistry Chemical Physics*, 4(1):134–145, 2002.

[29] Solomon, E. I., Heppner, D. E., Johnston, E. M., Ginsbach, J. W., Cirera, J., Qayyum, M., and Tian, L. Copper active sites in biology. *Chemical Reviews,* 114(7):3659–3853, 2014.

[30] van Lenthe, E., Wormer, P. E. and van der Avoird, A. D. Density functional calculations of molecular g–tensors in the zero–order regular approximation for relativistic effects. *The Journal of Chemical Physics*, 107(7):2488–2498, 1997.

[31] Schreckenbach, G. and Ziegler, T. Calculation of the g-tensor of electron paramagnetic resonance spectroscopy using gauge-including atomic orbitals and density functional theory. *The Journal of Physical Chemistry A*, 101(18):3388–3399, 1997.

[32] Neese, F. Prediction of electron paramagnetic resonance g values using coupled perturbed Hartree–Fock and Kohn–Sham theory. *The Journal of Chemical Physics*, 115(24):11080–11096, 2001.

[33] Malkina, O. L., Vaara, J., Schimmelpfennig, B., Munzarová, M., Malkin, V. G. and Kaupp, M. Density functional calculations of electronic g-tensors using spin-orbit pseudopotentials and mean-field all-electron spin-orbit operators. *Journal of the American Chemical Society*, 122(38):9206–9218, 2000.

[34] Hsiao, Y. W. and Zerner, M. C. Calculating ESR g tensors of doublet radicals by the semiempirical INDO/S method. *International Journal of Quantum Chemistry*, 75(4-5):577–584, 1999.

[35] Neese, F. Configuration interaction calculation of electronic g-tensors in transition metal complexes. *International Journal of Quantum Chemistry*, 83(3-4):104–114, 2001.

[36] Neese, F. and Solomon, E. I. Calculation of zero–field splittings, g-values, and the relativistic nephelauxetic effect in transition metal complexes. Application to high-spin ferric complexes. *Inorganic Chemistry*, 37(26):6568–6582, 1998.

[37] Peng, G., Nichols, J., McCullough Jr, E. A. and Spence, J. T. Models for the molybdenum (VI/V) centers of the molybdenum hydroxylases and related enzymes. Geometry, electronic structure, and EPR g-tensor predictions from ab initio and semiempirical molecular orbital studies. *Inorganic Chemistry*, 33(13):2857–2864, 1994.

[38] Neese, F., Wennmohs, F., Becker, U., Bykov, D., Ganyushin, D., Hansen, A. and Pantazis, D. A. *ORCA, Version 3.0.* Institute for physical and theoretical chemistry, Bonn, 2014

[39] Dolg, M., Wedig, U., Stoll, H. and Preuss, H. Energy-adjusted ab initio pseudopotentials for the first row transition elements, *The Journal of Chemical Physics*, 86(2):866, 1987.

[40] Andre, D., Hässermann, U., Dolg, M., Stoll, H. and Preuss, H. Energy-adjusted ab initio pseudopotentials for the second and third row transition elements. *Theoretical Chemistry Accounts*, 77:123–144, 1991.

[41] Weigend, F. and Ahlrichs, R. Balanced basis sets of split valance, triple zeta valance and quadruple zeta valence quality for H and Rn: Design and assessment of accuracy, *Physical Chemistry Chemical Physics*, 7:3297, 2005.

[42] Schäfer, A., Horn, H. And Ahlrichs, R. Fully optimized contracted gaussian basis sets for atoms Li to Kr, *The Journal of Chemical Physics*, 97:2571, 1992.

[43] Dutta, S. and Deka, R. C. Zero field splitting in Mn (III) complexes: a comparative study of DFT base coupled-perturbed and Pederson-khanna approaches. *Computational and Theoretical Chemistry*, 1072:1–6, 2015.

[44] Sim, F., St. Amant, A., Papai, I. and Salahub, D. R. Gaussian density functional calculations on hydrogen-bonded systems. *Journal of the American Chemical Society*, 114(11):4391-4400, 1992.

[45] Barone, V. in Chong, D. P., editor, *Recent Advances in Density Functional Methods*, Part I, World Scientific, Singapore, 1996.

[46] Rega, N., Cossi, M. and Barone, V. Development and validation of reliable quantum mechanical approaches for the study of free radicals in solution. *The Journal of Chemical Physics*, 105(24):11060–11067, 1996.

[47] Rega, N., Cossi, M. and Barone, V. Structure and magnetic properties of glycine radical in aqueous solution at different pH values. *Journal of the American Chemical Society*, 120(23):5723–5732, 1998.

[48] Adamo, C., Subra, R., Di Matteo, A. and Barone, V. Structure and magnetic properties of benzyl, anilino, and phenoxyl radicals by density functional computations. *The Journal of Chemical Physics*, 109(23):10244–10254, 1998..

[49] Filatov, M. In Schleyer, P. v. R. Allinger, N. L. Clark, T. Gasteiger, J. Kollman, P. A. Schaefer III, H. F. and Schreiner, P. R. *Encyclopedia of Computational Chemistry,* Wiley, Chichester, 2003.

[50] M. Filatov, On representation of the Hamiltonian matrix elements in relativistic regular approximation, *The Journal of Physical Chemistry Letters*, 365:222, 2002.

[51] M. Filatov and D. Cremer, Analytic energy derivatives for regular approximations of relativistic effects applicable to methods with and without correction correlations, *The Journal of Chemical Physics,* 118:6741, 2003.

[52] Dyall, K. G. And Lenthe, E. Van. Relativistic regular approximations revisited: an infinite order relativistic approximation, *The Journal of Chemical Physics*, 111:1366, 1999.

[53] Reiher, M. And Wolf, A. *Relativistic Quantum Chemistry: The Fundamental Theory of Molecular Science*, Wiley VCH, 2nd edition, 2014.

[54] Dyall, K. G. Interfacing relativistic and nonrelativistic methods. I. Normalized elimination of the small component in the modified Dirac equation, *The Journal of Chemical Physics*, 106:9618, 1997.